Received: 25 May 2021 | Revised: 26 October 2021 | Accepted: 5 November 2021

DOI: 10.1002/hep.32232

ORIGINAL ARTICLE

IL-6–induced cGGNBP2 encodes a protein to promote cell growth and metastasis in intrahepatic cholangiocarcinoma

Hui Li[1,2,3] | **Tian Lan**[1,2] | **Hailing Liu**[1,2] | **Chang Liu**[1] | **Junlong Dai**[1] | **Lin Xu**[2] | **Yunshi Cai**[1,2] | **Guimin Hou**[1,2] | **Kunlin Xie**[1,2] | **Mingheng Liao**[1,2] | **Jiaxin Li**[1,2] | **Jiwei Huang**[1,2] | **Kefei Yuan**[1,2] | **Genshu Wang**[4] | **Yong Zeng**[1,2] | **Hong Wu**[1,2]

[1]Department of Liver Surgery, Liver Transplantation Division, West China Hospital, Sichuan University, Chengdu, China

[2]Laboratory of Liver Surgery, West China Hospital, Sichuan University, Chengdu, China

[3]Department of Hepatobiliary Pancreatic Tumor Center, Chongqing University Cancer Hospital, Chongqing, China

[4]Department of Hepatic Surgery and Liver Transplantation Center, The Third Affiliated Hospital of Sun Yat-sen University, Guangzhou, China

Correspondence
Kefei Yuan, Yong Zeng, and Hong Wu, Department of Liver Surgery, Liver Transplantation Division, Laboratory of Liver Surgery, West China Hospital, Sichuan University, No. 37 of Guoxue Lane, Wuhou District, Chengdu 610041, China.
Email: ykf13@163.com, zeng_y@scu.edu.cn, and wuhong@scu.edu.cn

Genshu Wang, Department of Hepatic Surgery and Liver Transplantation Center, The Third Affiliated Hospital of Sun Yat-sen University, No. 600 of Tianhe Road, Guangzhou 510006, China.
Email: wgsh168@163.com

Funding information
This work was supported by grants from the National Key Technologies R&D Program (2018YFC1106800), the National Natural Science Foundation of China (82173248, 81972747, 81972204, 81872004, 81800564, 81770615, 81702327, 81700555, and 81672882), the Science and Technology Support Program of Sichuan Province (2019YFQ0001, 2018SZ0115, and 2017SZ0003), the Science and Technology Program of Tibet Autonomous Region (XZ201801-GB-02), and the 1.3.5 project for disciplines of excellence, West China Hospital, Sichuan University (ZYJC18008)

Abstract

Background and Aims: IL-6–induced tumor progression has been well established through the induction of antiapoptotic and proliferative genes. However, whether other mechanisms such as IL-6 regulation of circular RNAs (circRNAs) may also contribute to tumor development remains unknown.

Approach and Results: High-throughput RNA sequencing was used to identify the differentially expressed circRNAs on IL-6 stimulation in intrahepatic cholangiocarcinoma (ICC) cells. CircRNA GGNBP2 (derived from *ggnbp2* gene, termed as cGGNBP2) was up-regulated by IL-6 treatment in a time and concentration-dependent manner. The biogenesis of cGGNBP2 was regulated by RNA-binding protein DEx-H Box Helicase 9, which was also mediated by IL-6 exposure. Mass spectrometry and western blotting identified a protein cGGNBP2-184aa encoded by cGGNBP2. cGGNBP2-184aa promoted ICC cell proliferation and metastasis in vitro and in vivo. Mechanistically, cGGNBP2-184aa directly interacted with signal transducers and activators of transduction-3 (STAT3), phosphorylated $STAT3^{Tyr705}$, and played a positive regulatory role in modulating IL-6/STAT3 signaling. IL-6/cGGNBP2-184aa/STAT3 formed a positive feedback loop to sustain constitutive activation of IL-6/STAT3 signaling.

Abbreviations: CAF, cancer-associated fibroblast; cGGNBP2, circular RNA derived from exons 4-6 of the *ggnbp2* gene; cGGNBP2-184aa, specific protein encoded by cGGNBP2; circRNA, circular RNA; co-IP, co-immunoprecipitation; DBD, DNA binding domain; DHX9, DExH-Box Helicase 9; FRCM, forward RCM; HA, hemagglutinin; ICC, intrahepatic cholangiocarcinoma; IL-6R, IL-6 receptor; IRES, internal ribosome entry site; JAK, Janus kinase; ORF, open reading frame; OS, overall survival; qRT-PCR, quantitative reverse transcription PCR; RBP, RNA-binding protein; RCM, reverse complementary match; RFS, recurrence-free survival; RNA-seq, RNA sequencing; RRCM, reverse RCM; shRNA, short hairpin RNA; siRNA, small interfering RNA; STAT3, signal transducers and activators of transduction-3; TIL, tumor-infiltrating lymphocyte.

Hui Li, Tian Lan, and Hailing Liu contributed equally to this work.

Elevated cGGNBP2 expression was correlated with poor prognosis of patients with ICC and was identified as an independent risk factor for patient prognosis. **Conclusions:** Our study demonstrates that cGGNBP2-184aa, a protein encoded by IL-6–induced cGGNBP2, formed a positive feedback loop to facilitate ICC progression and may serve as an auxiliary target for clinical IL-6/STAT3-targeting treatments in ICC.

INTRODUCTION

Intrahepatic cholangiocarcinoma (ICC) accounts for approximately 10%-15% of primary liver cancer, and the morbidity assumes a notable uptrend in high-income countries in recent years.[1,2] The prognosis of ICC remains poor due to the frequent metastasis and rapid postsurgical recurrence.[3] It is known that metastasis is the outcome of a complex signaling network and depends on cell-intrinsic properties and specific microenvironment of cancer cells.[4] However, the precise molecular mechanisms underlying ICC metastatic cascade remain poorly understood. Therefore, advancing our understanding of pivotal cancer-promoting events may contribute to the development of effective metastasis-targeted treatments and improve the prognosis of patients with ICC.

The relation between inflammation and cancer has been increasingly appreciated.[5] IL-6, a pleiotropic cytokine produced in response to stress and infection in the presence of inflammatory stimuli, plays an important role in tumorigenesis and cancer progression. Aberrant IL-6 expression, a consequence of chronic inflammation in tumor microenvironment, could promote tumor cell growth and metastasis through activation of the downstream signaling in which signal transducers and activators of transduction-3 (STAT3) were phosphorylated and translocated to nucleus to initiate the transcription of the target genes. Aside from the classic IL-6/STAT3 signaling axis, previous studies have reported that IL-6 could induce the expression of long noncoding RNAs to promote tumor aggressiveness.[6] Hence, molecular therapies targeting IL-6/STAT3 pathway components necessitate a better understanding of specific downstream effectors.

Circular RNAs (circRNAs), an abundant class of covalently closed and single-stranded transcripts, are involved in multiple physiological and pathological processes.[7] Currently, only a limited number of circRNAs have been confirmed as functional molecules in biological processes, such as cell proliferation, migration, and invasion.[8] Conventionally, circRNAs were considered as noncoding RNAs because of a lack of 5′cap as well as 3′end structure and exerted their functions mainly as microRNA sponge and protein scaffold.[9,10] However, recent studies have revealed that circRNAs could recruit ribosomes and were associated with putative open reading frame (ORF), suggesting an unexpected protein-coding potential.[11] Internal ribosome entry site (IRES)-induced protein translation was found to be a mechanism of circRNA-mediated translation, which is independent of 5′cap structure.[12] These circRNA-encoded proteins were shown to regulate important hallmarks, including tumorigenesis and metastasis in cancers.[13] Nevertheless, whether circRNAs play specific roles in cancer-related inflammation remains unclear. In this study, we identified an IL-6–induced circRNA (a circRNA derived from exon 3-6 of the gametogenetin-binding protein 2, which we have termed cGGNBP2). Furthermore, we characterized the protein (cGGNBP2-184aa) it encoded and investigated the role of cGGNBP2-184aa in IL-6/STAT3 signaling and ICC metastasis.

PATIENTS AND METHODS

Patient cohorts and tissues

Tumor tissues were obtained from surgical specimen archives of 136 patients with ICC at West China Hospital from 2009 to 2018. Frozen tissues were used for quantitative reverse transcription PCR (qRT-PCR) and western blotting analyses, whereas formalin-fixed and paraffin-embedded tissues were used for immunohistochemistry analyses. Of these, 40 patients were tested for preoperative serum IL-6 levels. Human tissues and relative clinical data collection conformed to the ethical guidelines of the 1975 Declaration of Helsinki and approved by the Ethics Committee of West China Hospital.

RNA sequencing

Total RNAs were extracted using Trizol Reagent. The high-throughput sequencing and analyses for circRNAs were carried out by Novogene Technology Co., Ltd. The clustering of the index-coded samples was performed on a cBot Cluster Generation System using TruSeq PE Cluster Kit v3-cBot-HS (Illumina) according to the manufacturer's instructions. After cluster generation, the libraries were sequenced on an Illumina Hiseq 4000 platform.

The circRNAs were detected and identified using find_circ.[7] Total RNAs of indicated cells were used for mRNA sequencing on an Illumina Novaseq 6000 platform at the LC-BIO Bio-tech Ltd. Gene set enrichment analysis (GSEA) was applied for pathway analysis.

In vivo xenograft assays

For subcutaneous xenograft models, 2×10^6 cells were injected subcutaneously into the right axilla of mice. For liver orthotopic-implanted models, 1×10^6 cells were transplanted into the left lobes of the liver. For lung metastasis models, 2×10^6 cells were injected through tail veins. All animals received humane care according to the criteria outlined in the NIH Guide for the Care and Use of Laboratory Animals. The in vivo animal experiments were approved by the Animal Ethics Committees of West China Hospital.

Statistical analysis

All experiments were performed at least three times unless otherwise noted. Comparisons were performed using Student *t* test, one-way ANOVA, or Mann-Whitney U test, as appropriate. A two-tailed p value < 0.05 was considered statistically significant. All statistical analyses were carried out by applying SPSS (version 23.0, SPSS Inc.), GraphPad Prism (version 8.0), or MedCalc software (version 15.2.2).

For detailed materials and methods, please refer to Supporting Information.

RESULTS

cGGNBP2 is up-regulated by IL-6 and is clinically relevant to prognosis of patients with ICC

Serum IL-6 has been shown to correlate with the prognosis of different cancers, including liver cancer.[14,15] We firstly investigated prognostic value of serum IL-6 in ICC, showing that elevated serum IL-6 level was significantly correlated with larger tumor size, multiple tumor number, lymph node invasion, and poor prognosis (Table S1, Figure S1). To determine the underlying molecular mechanisms in this process, we treated ICC cells (RBE cell line) with IL-6 at different concentrations and time points. The cells showed increased invasive capability, as indicated by the increased spindle-shaped appearance along with the rise of IL-6 concentration (Figure S2A,B). IL-6 treatment also strengthened the invasive capability of HuccT1 cells but not normal cholangiocytes (human intrahepatic biliary epithelial cell) (Figure S2C,D). We then used RNA sequencing (RNA-seq) analysis to establish circRNA expression profiles in IL-6–treated RBE cells (Figure 1A). A total of 3,951 distinct circRNAs were identified, among which 3,055 have been identified in the circBase (Figure 1B) and 3,737 (94.6%) consisted of exons (Figure S2E,F). Of the identified circRNAs, nine were significantly up-regulated and seven were down-regulated by IL-6 treatment (Table S2).

To validate the RNA-seq results, we performed qRT-PCR for the nine up-regulated circRNAs. Sanger sequencing of PCR products confirmed the back-splice junctions of candidate circRNAs (Figure S2G,H). Furthermore, no significant changes were found in these circRNAs after treatment with RNase R (Figure S2I, Figure S3A). We then measured the relative expression of these circRNAs in RBE cells treated with IL-6. Among them, circRNA GGNBP2 (hsa_circ_0003930, cGGNBP2), a circRNA derived from exon 3-6 of the gametogenetin-binding protein 2 (*ggnbp2*) gene at chromosome 17q12, was found to be the most highly up-regulated in IL-6–treated cells (Figure 1C,D). The divergent and convergent primers, oligo $(dT)_{18}$ primers, and actinomycin D were used to confirm the circularity of cGGNBP2 (Figure S3B-D). The expression of cGGNBP2 in RBE cells peaked at a concentration of 50 ng/ml and 24 hours after IL-6 treatment (Figure 1E). Additionally, the fluorescent *in situ* hybridization and subcellular RNA fractionation showed that cGGNBP2 was located primarily in cytoplasm, suggesting that cGGNBP2 may exert its biological function there (Figure 1F, Figure S3E).

FIGURE 1 cGGNBP2 is up-regulated by IL-6 and serves as a prognostic indicator of ICC. (A) Clustered heat map representation of differentially expressed circRNAs in RBE cells treated with IL-6 (50 ng/ml) for 24 hours and the control cells treated with PBS. (B) The 3,055 circRNAs in our data were identified with circBase records. (C) qRT-PCR validated the top nine up-regulated circRNAs in RBE cells treated with IL-6 compared with those with PBS. (D) Scheme illustrating the genomic locus and production of cGGNBP2. The special primers used for detection of cGGNBP2 by qRT-PCR are indicated by red arrows and validated by Sanger sequencing. (E) Left: the relative RNA levels of cGGNBP2 were evaluated after treatment with IL-6 at the indicated concentration. Right: the relative cGGNBP2 levels were assessed by qRT-PCR after treatment with IL-6 (50 ng/ml) at the indicated time point. (F) RNA fluorescence *in situ* hybridization showing cytoplasmic localization of cGGNBP2 and relative expression of cGGNBP2 after treatment with IL-6 in RBE and HuccT1 cells. Antisense cGGNBP2 was used as negative control. The 18S and U6 were applied as positive controls in the cytoplasm and nucleus. Scale bar, 10 μm. (G) Left: the correlation between the relative cGGNBP2 expression of tumor tissues and serum IL-6 level in 40 patients with ICC; right: the correlation between the relative cGGNBP2 expression and relative IL-6R expression of tumor tissues in 136 patients with ICC. (H) Kaplan-Meier survival analysis showing the correlation between relative cGGNBP2 expression of ICC tissues and OS or RFS. The cutoff value of serum IL-6 was determined by X-tile. p values were determined by log-rank tests. (I) Multivariate analyses showing prognostic indicators for OS and RFS. AS, probe for antisense cGGNBP2; mGGNBP2, the mRNA of GGNBP2. *p < 0.05; **p < 0.01; ***p < 0.001

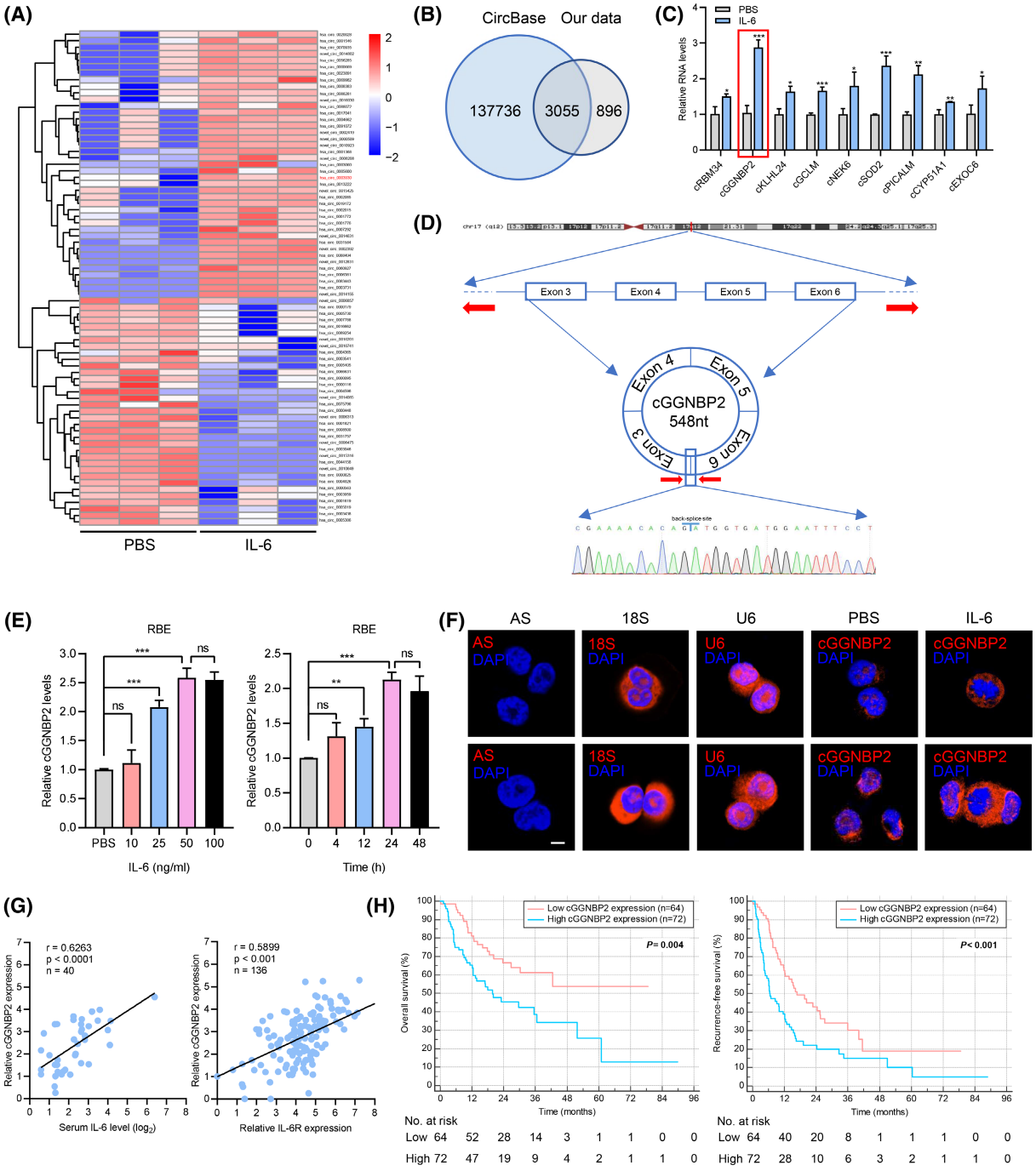

To further determine the clinical relevance of cGGNBP2, the expression levels of cGGNBP2 were evaluated in 136 matched ICC and adjacent nontumor samples. The results demonstrated a much higher expression level of cGGNBP2 in tumor than in nontumor (Figure S3F). Moreover, there is a strong positive correlation between cGGNBP2 expression level of tumor and serum IL-6 level (Figure 1G). However, the cGGNBP2 expression showed no significant difference between patients with ICC and those with

TABLE 1 Baseline characteristics of 136 patients with ICC according to cGGNBP2 expression levels

Variables	Low cGGNBP2 (*n* = 64)	High cGGNBP2 (*n* = 72)	*p* value
Age, year, >60/≤60	25/39	34/38	0.388
Sex, female/male	27/37	36/36	0.393
HbsAg, positive/negative	18/46	17/55	0.583
Hepatolithiasis, present/absent	4/60	8/64	0.376
CA19-9, >22/≤22	30/34	54/18	0.001
Tumor size, cm, >5/≤5	26/38	52/20	<0.001
Tumor number, multiple/solitary	14/50	30/42	0.017
Differentiation, poor/well-moderate	13/51	22/50	0.238
Microvascular invasion, present/absent	6/58	9/63	0.596
Lymph node, positive/negative	7/57	18/54	0.046
Cirrhosis, with/without	45/19	52/20	0.851
TNM stage, III/I-II	31/33	53/19	0.003

Abbreviation: TNM, tumor-node-metastasis.

hepatic hemangioma with comparable serum IL-6 levels (Figure S3G). Because ICC is enriched of stroma and cancer-associated fibroblasts (CAFs), we then evaluated the cGGNBP2 expression of ICC cells, noncancerous cholangiocytes and CAFs in 20 freshly isolated tissues. The results showed that the cGGNBP2 expression was extremely low in CAFs. In addition, a much higher cGGNBP2 expression was observed in ICC cells compared with noncancerous cholangiocytes (Figure S3H). Additionally, the expression of cGGNBP2 was positively correlative with the expression of IL-6 receptor (IL-6R) as well as IL-6 in tumor tissues (Figure 1G, Figure S3I,J). After knocking down IL-6R, the cGGNBP2 expression was down-regulated in ICC cells (Figure S3K). Furthermore, cGGNBP2 could not be up-regulated by IL-6 treatment in cells with IL-6R depletion (Figure S3L). We then examined the potential association between cGGNBP2 expression and clinicopathological characteristics as well as patient prognosis. An elevated cGGNBP2 expression was significantly associated with increased serum carbohydrate antigen 19-9 level, larger tumor size, more tumor numbers, presence of lymph node metastasis, and more advanced tumor stage, indicating that cGGNBP2 was correlated to ICC progression (Table 1). Further Kaplan-Meier survival analyses demonstrated that patients with ICC with higher cGGNBP2 expression were associated with shorter overall survival (OS) and recurrence-free survival (RFS) after curative resection (Figure 1H). In the Cox proportional hazards regression models, elevated cGGNBP2 expression was identified as an independent risk factor for OS and RFS (Figure 1I, Table S4). Collectively, our data demonstrated that cGGNBP2 is up-regulated by IL-6 and may serve as a prognostic factor for patients with ICC.

DExH-box helicase 9 regulates the expression of cGGNBP2

It has been reported that some RNA-binding proteins (RBPs) were involved in circRNA biogenesis by binding to specific sequences to regulate the back splicing of circRNAs.[16-18] To investigate whether RBPs were involved in the formation of cGGNBP2, we performed RNA-seq to analyze the expression profile of 11 RBPs, which have previously been reported to affect circRNA

FIGURE 2 DHX9 regulates the expression of cGGNBP2 through binding to their flanking inverted complementary sequences. (A) RNA-seq analysis of expression profiles of 11 RBPs after treatment with IL-6 in RBE cells. (B) qRT-PCR of the relative mRNA expression of DHX9 in RBE and HuccT1 cells treated with IL-6 or PBS. (C) Western blotting (WB) analysis of the relative protein expression of DHX9 in RBE and HuccT1 cells treated with IL-6 or PBS. (D) Left: Representative immunohistochemistry staining images of DHX9 with relatively low or high expression in ICC tissues. Right: The correlation between the immunohistochemistry staining scores of DHX9 in tumor tissues and serum IL-6 levels in 40 patients with ICC (top); the correlation between DHX9 and relative cGGNBP2 expression in tumor tissues of 136 patients with ICC (bottom). (E) Top: qRT-PCR for cGGNBP2 expression in DHX9-depleted RBE and HuccT1 cells. Bottom: WB analysis for relative DHX9 protein expression in DHX9-depleted RBE and HuccT1 cells. (F) Schematic of five types of vectors (#1 to #5). The genomic region for cGGNBP2 (exon 3-6) with its wild-type (wt) flanking inverted complementary sequences (red boxes) was inserted into vector (#2). #3 to #5 represent a series of deletions of flanking inverted complementary sequences. The northern blotting (NB) probe targeting cGGNBP2 is indicated by the dotted line. (G, H) qRT-PCR and NB analysis of relative cGGNBP2 expression in HEK-293T cells transfected with five types of vectors. (I) RNA immunoprecipitation assays showed DHX9 bind to flanking inverted complementary sequences. IgG was used as a control. (J) qRT-PCR analysis showed relative cGGNBP2 expression in indicated cells after transfection with vectors and treatment with IL-6. FRCM in intron 2; RRCM in intron 6. $^{**}p < 0.01$; $^{***}p < 0.001$; ns, not significant

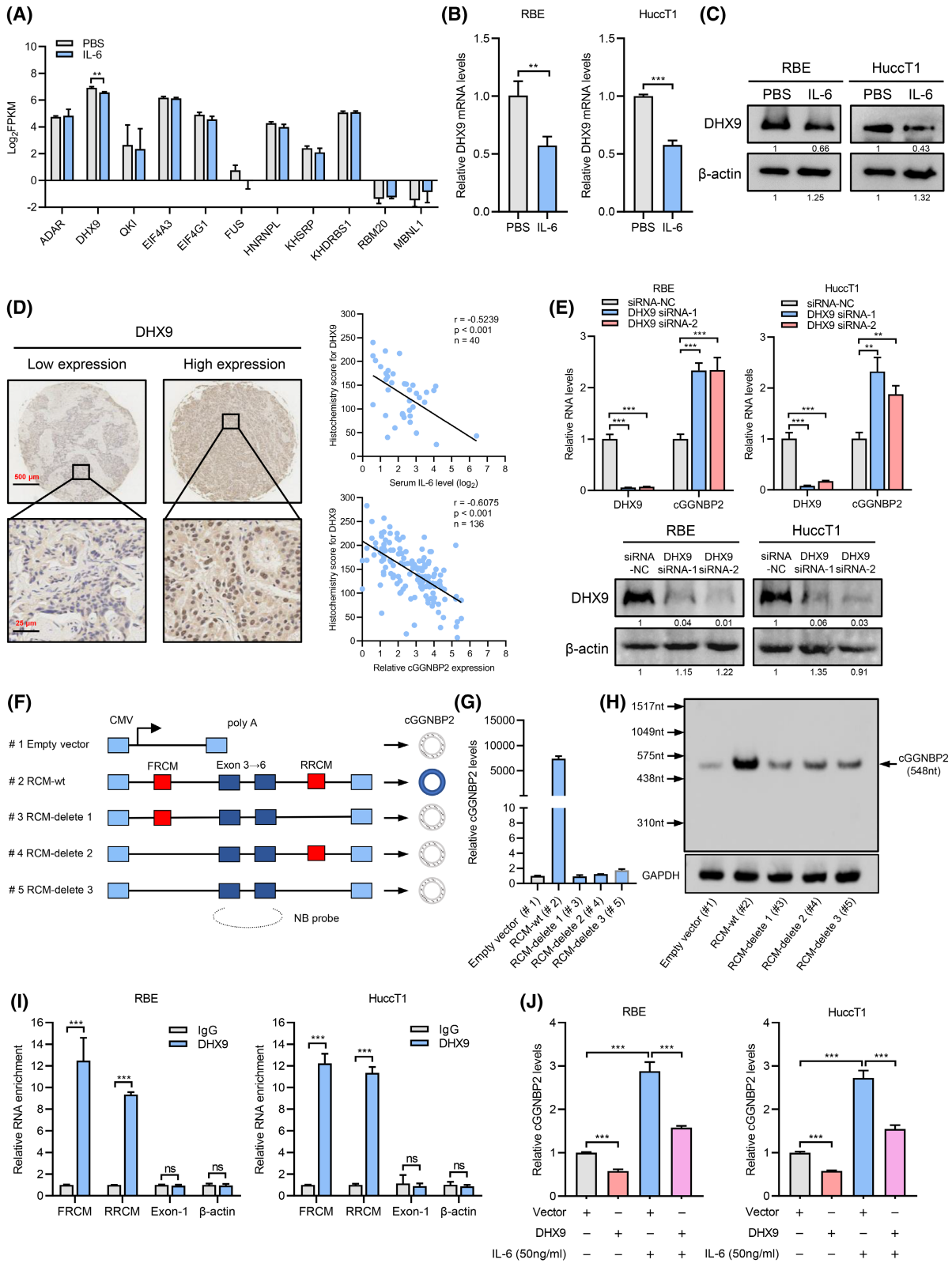

genesis, in IL-6–treated cells. Our data demonstrated that the expression of DExH-Box Helicase 9 (DHX9) was significantly altered after IL-6 treatment (Figure 2A, Table S5). To confirm the RNA-seq results, we treated RBE and HuccT1 cells with IL-6 and measured the mRNA and protein expression level of DHX9. The results confirmed that DHX9 could be down-regulated by IL-6 (Figure 2B,C). Furthermore, the expression of DHX9 in tumor tissue was negatively related to serum IL-6 level in 40 patients with ICC. Additionally, the cGGNBP2

expression was also negatively correlated to the histochemistry score of DHX9 in 136 ICC tissues (Figure 2D). After silencing of DHX9, cGGNBP2 expression level could be significantly up-regulated (Figure 2E).

Accumulating evidence have shown that complementary sequences in flanking introns, like Alu repeat elements or other nonrepetitive complementary sequences, facilitated circRNA formation.[19] The efficiency of circRNA circularization, especially exon-derived ones, can be regulated by RBPs-mediated RNA pairing across flanking introns.[18,20] To explore the mechanisms of cGGNBP2 circularization, we examined the sequences of flanking introns of cGGNBP2 and found highly reverse complementary sequences between intron 2 and intron 6 (79% identity among 301 nucleotides; Figure S4A). To further test whether cGGNBP2 was regulated by the reverse complementary match (RCM), a wild-type plasmid (a 1,915-nt region spanning from forward RCM [FRCM] of intron 2 to reverse RCM of intron 6, #2) and three deletion mutants (#3-5) were constructed (Figure 2F). After transfection with these vectors, qRT-PCR results showed that cGGNBP2 expression was only up-regulated in cells transfected with RCM-wt vector, indicating that both FRCM and reverse RCM (RRCM) were necessary for cGGNBP2 biogenesis (Figure 2G). This result was further confirmed by northern blotting (Figure 2H).

We hypothesized that DHX9 bound to the RCM of cGGNBP2 within the pre-mRNA transcript of *ggnbp2* gene in the nucleus and thereby inhibited its circularization. To test our hypothesis, RNA immunoprecipitation was performed using an antibody against DHX9. As expected, the FRCM and RRCM could be significantly enriched, whereas exon 1 of *ggnbp2* gene could not (Figure 2I). In addition, we overexpressed DHX9 in cells transfected with five RCM-related vectors and found a general down-regulation after DHX9 overexpression (Figure S4B,C). Subsequently, we treated DHX9-depletion or DHX9-overexpressing ICC cells with IL-6 and found that the cGGNBP2 expression could not be further up-regulated in the absence of DHX9 (Figure S4D), whereas up-regulation cGGNBP2 by IL-6 could be abolished by DHX9 overexpression (Figure S4E, Figure 2J). Taken together, we found that IL-6 treatment down-regulates DHX9 expression. More importantly, reduced DHX9 could enhance cGGNBP2 expression in posttranscriptional process through promoting RNA pairing by binding to the flanking intronic complementary sequences of cGGNBP2.

cGGNBP2 promotes ICC cell growth and metastasis in vitro and in vivo

To elucidate the biological function of cGGNBP2 in ICC cell growth and metastasis, we knocked down cGGNBP2 by small interfering RNA (siRNA) targeting back-splice sequences in Hccc9810 and HuccT1 cells and overexpressed cGGNBP2 using RCM-wt vector in RBE and HuccT1 cells without disturbing the mRNA of GGNBP2 and pre-mRNA of GGNBP2 (Figure S5A-D). cGGNBP2 knockdown markedly suppressed cell proliferation, cell cycle, and cell invasive capacity, whereas overexpression of cGGNBP2 had the opposite effects (Figures S6 and S7). Moreover, cGGNBP2 knockdown could abolish most of the effect of IL-6 on facilitating ICC cell proliferation and invasion (Figure S8A-C).

Next, we explored cGGNBP2 function in vivo. cGGNBP2 was stably knocked down by short hairpin RNA (GGNBP2 shRNA) in HuccT1 cells and overexpressed in RBE and HuccT1 cells, followed by subcutaneous implantation into nude mice. Tumor growth was significantly inhibited by cGGNBP2 silencing and accelerated by overexpression of cGGNBP2 (Figures S9A,B and S10A). We further established liver orthotopic-implantation and lung metastasis models to evaluate the role of cGGNBP2 on tumor metastasis. As a result, fewer intrahepatic metastatic foci were observed in livers following cGGNBP2 knockdown (Figure S9C). Conversely, enhanced cGGNBP2 facilitated intrahepatic metastasis (Figures S9D and S10B). Similarly, loss of cGGNBP2 repressed the formation of lung metastases, whereas ectopic cGGNBP2 expression promoted lung metastases (Figures S9E,F and S10C). Taken together, these results suggested a functional role of cGGNBP2 in facilitating ICC cell growth and metastasis in vitro and in vivo.

FIGURE 3 cGGNBP2 encodes a protein termed as cGGNBP2-184aa. (A) Top: The putative ORF and its location in the genomic region of cGGNBP2. Bottom: The sequences of the putative ORF. Red sequence represents unique amino acid encoded by cGGNBP2-184aa. (B) Left: The schematic of five types of vectors used for luciferase reporter assays. Wild-type (WT) or a series of deletions of IRES sequences were inserted into vectors (#1 to #4). #5 represents a vector inserted with mutated IRES sequences (IRES-MUT). Right: The relative luciferase activity of FLuc/Rluc in the indicated five vectors. FLuc, firefly luciferase; RLuc, renilla luciferase. (C) Top: Total proteins from RBE cells transfected with control or cGGNBP2-overexpression plasmid were separated through SDS-PAGE (left). The cGGNBP2-184aa overexpression was confirmed by western blotting (WB) assay using a specific antibody against the amino acid sequences of cGGNBP2-184aa (right). Bottom: The differential gel bands near 26 kD were cut and subjected to liquid chromatography–tandem mass spectrometry. The cGGNBP2-184aa was identified. (D) WB assays showing the relative cGGNBP2-184aa expression in RBE and HuccT1 cells after treatment with IL-6 (50 ng/ml for 24 hours). (E) WB assays showing the relative cGGNBP2-184aa expression in indicated cells treated with IL-6 or not. (F) Immunofluorescence (IF) assays showing the cytoplasmic cellular localization of cGGNBP2-184aa in RBE and HuccT1 cells transfected with Vector or HA-tagged cGGNBP2-184aa plasmids, detected using anti-HA antibody. Scale bar, 10 μm. (G) Subcellular fractionation assays identified the cytoplasmic cellular localization of cGGNBP2-184aa in the indicated cells transfected with HA-tagged cGGNBP2-184aa plasmids. GAPDH and H3 were used as positive controls in the cytoplasm and nucleus, respectively

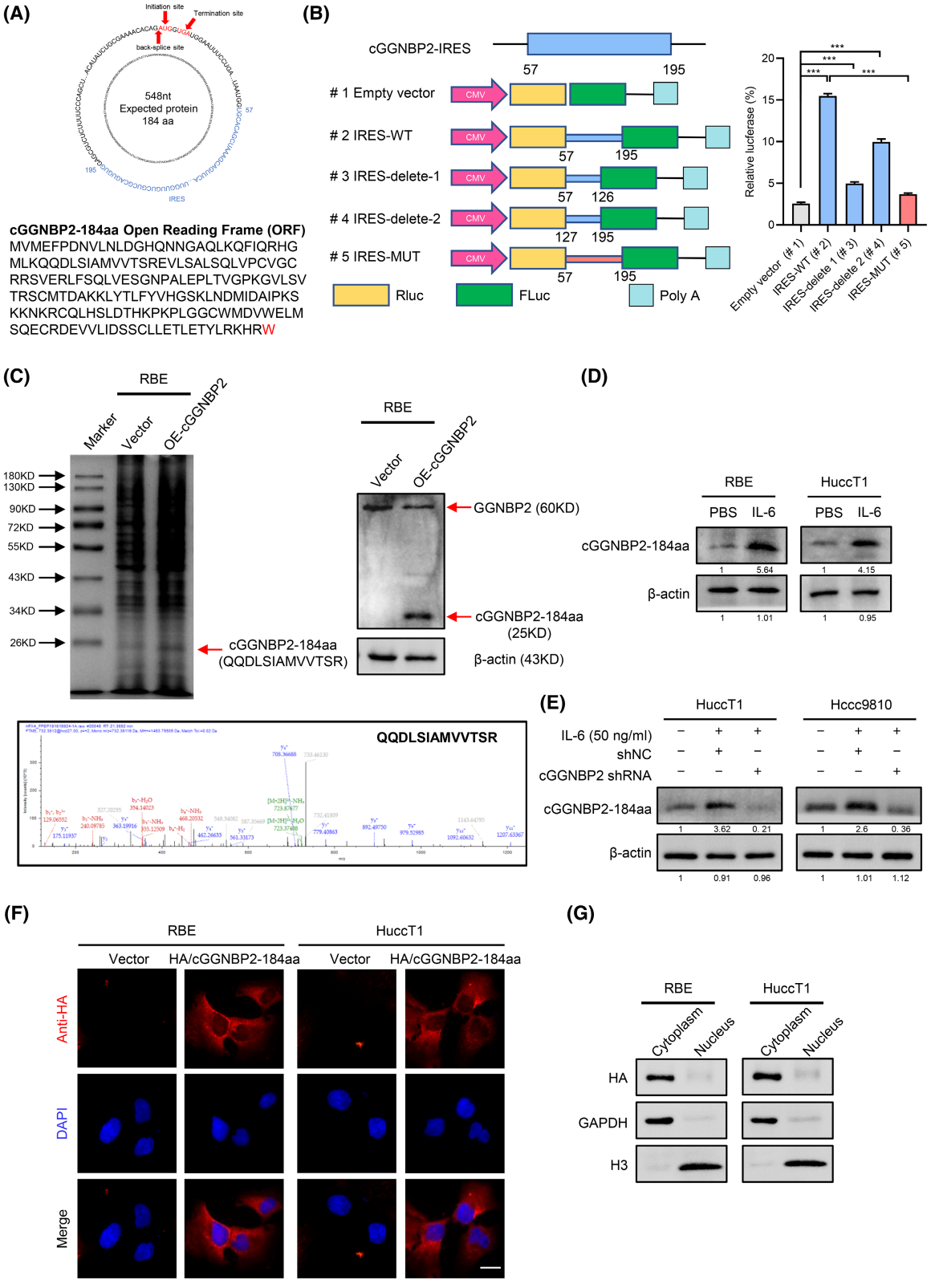

cGGNBP2 encodes a 184 amino acid protein

Recent studies have demonstrated that some circRNAs encoded functional peptides.[21,22] To examine the protein-coding potential of cGGNBP2, we first analyzed the putative ORF and IRES of cGGNBP2 as annotated in circRNADb.[23] A highly conserved ORF with the potential of encoding a 184aa-protein was detected (Figure S11A, Figure 3A). As IRES was essential for

5′cap-lacking circRNA to recruit ribosomes to initiate translation, we next tested the function of predicted IRES in cGGNBP2 using dual-luciferase assays (Figure 3B). Wild-type or truncated IRES sequences were cloned between tandem Renilla and Firefly luciferase reporters with independent initiation and termination codons (Figure S11B). Wild-type IRES and IRES-delete 1 showed the highest and the lowest luciferase activity, indicating the function of IRES was predominately determined by the downstream sequences. When the IRES was mutated and cloned into a dual-luciferase vector, luciferase activity was markedly reduced, further supporting a functional role of the IRES in initiating 5′cap-independent translation (Figure S11C). Driven by this IRES, a predicted protein consisted of 184 amino acids (termed cGGNBP2-184aa) could be translated by cGGNBP2 (Figure 3A). As predicted, an enhanced band could be observed after cGGNBP2 overexpression compared with the control vector on a SDS-PAGE gel. Subsequent mass spectrometry confirmed that the amino acid sequences were highly aligned to the putative sequences of cGGNBP2-184aa (Figure 3C, left).

To further characterize cGGNBP2-184aa, we generated a highly specific antibody against the amino acid sequences (KKNKRCQLHSLDTHKPK) of cGGNBP2-184aa, which was supposed to recognize both GGNBP2 and cGGNBP2-184aa. Importantly, the expression of cGGNBP2-184aa was drastically up-regulated after cGGNBP2 overexpression, whereas GGNBP2 expression level showed no significant change (Figure 3C, right). Consistent with the expression of cGGNBP2, cGGNBP2-184aa could be up-regulated by IL-6 stimuli in a concentration and time-dependent manner (Figure 3D, Figure S12A). Knockdown of DHX9 enhanced cGGNBP2-184aa expression (Figure S12B). Furthermore, silencing cGGNBP2 abolished the IL-6–mediated enhanced cGGNBP2-184aa expression (Figure 3E). These results demonstrated that cGGNBP2 encodes a protein, cGGNBP2-184aa.

cGGNBP2-184aa promotes ICC cell growth and metastasis in vitro

To investigate the function of cGGNBP2-184aa, we first examined cGGNBP2-184aa expression in ICC cell lines. Consistent with cGGNBP2, cGGNBP2-184aa expression was highest in Hccc9810 cells and lowest in RBE cells (Figure S12C). The ORF of cGGNBP2-184aa was then cloned into an expression vector. A mutated IRES (IRES-MUT) vector was also constructed by mutating IRES within the OE-cGGNBP2 plasmid (Figure S12D). Following transfecting hemagglutinin (HA)-labeled cGGNBP2-184aa plasmid into ICC cells, it was clear that cGGNBP2-184aa was mainly located in the cytoplasm by immunofluorescence using an anti-HA antibody and subcellular protein fractionation (Figure 3F,G).

Next, we established stable cell lines by lentiviral infection. cGGNBP2 expression was dramatically enhanced by IRES-MUT, whereas cGGNBP2-184aa expression did not show significant change. Conversely, overexpression of cGGNBP2-184aa ORF enhanced cGGNBP2-184aa expression but not cGGNBP2 (Figure S12E, Figure 4A). Additionally, overexpression of cGGNBP2-184aa ORF restored cGGNBP2-184aa protein expression that was knocked down by a cGGNBP2 shRNA, whereas cGGNBP2 RNA expression remained unchanged (Figure S12F, Figure 4I). As expected, up-regulation of cGGNBP2-184aa expression but not IRES-MUT cGGNBP2 expression promoted ICC cell proliferation, cell cycle, and invasion capacity, whereas inhibited apoptotic program (Figure 4B-H, Figure S13A,C). Overexpression of cGGNBP2-184aa ORF abolished the inhibitory effect of cGGNBP2 shRNA on proliferation, cell cycle, and invasion capacity (Figures 4J-P and 13B). Taken together, cGGNBP2 encoded cGGNBP2-184aa to facilitate ICC cell proliferation and metastasis in vitro.

cGGNBP2-184aa facilitates STAT3 phosphorylation in ICC cells

To further elucidate the mechanism underlying cGGNBP2-184aa–induced ICC cell growth and metastasis, RNAs were extracted from cells with overexpression of IRES-MUT and OE-cGGNBP2 and subjected to RNA-seq. A total of 292 up-regulated and 240 down-regulated genes were differentially expressed (Figure S14A). Janus kinase (JAK)-STAT signaling pathway was significantly altered by cGGNBP2-184aa overexpression based on Kyoto Encyclopedia of Genes and Genomes enrichment analysis (Figure 5A), whereas GSEA also demonstrated that cGGNBP2-184aa overexpression positively affected JAK-STAT pathway and cell cycle process (Figure S14B).

STAT3, the primary molecule of JAK-STAT pathway, is a key transcription factor that shows a critical effect on the progression of diverse human cancers.[24,25] Because phosphorylation is required for STAT3 nuclear translocation and transcriptional activity,[26] we then investigated whether cGGNBP2-184aa regulated STAT3 phosphorylation. Ectopic cGGNBP2-184aa expression significantly enhanced the phosphorylation of STAT3 at Tyr705 and total STAT3 protein level in RBE cells (Figure 5B). In addition, inhibition of $STAT3^{Tyr705}$ phosphorylation by cGGNBP2-184aa deficiency could be rescued by overexpression of cGGNBP2-184aa ORF in HuccT1 cells (Figure 5C). However, $STAT3^{Ser727}$ phosphorylation was not influenced by the change of cGGNBP2-184aa expression. Next, to examine the translocation of STAT3, we performed subcellular protein fraction assay. cGGNBP2-184aa overexpression significantly accelerated nuclear translocation of

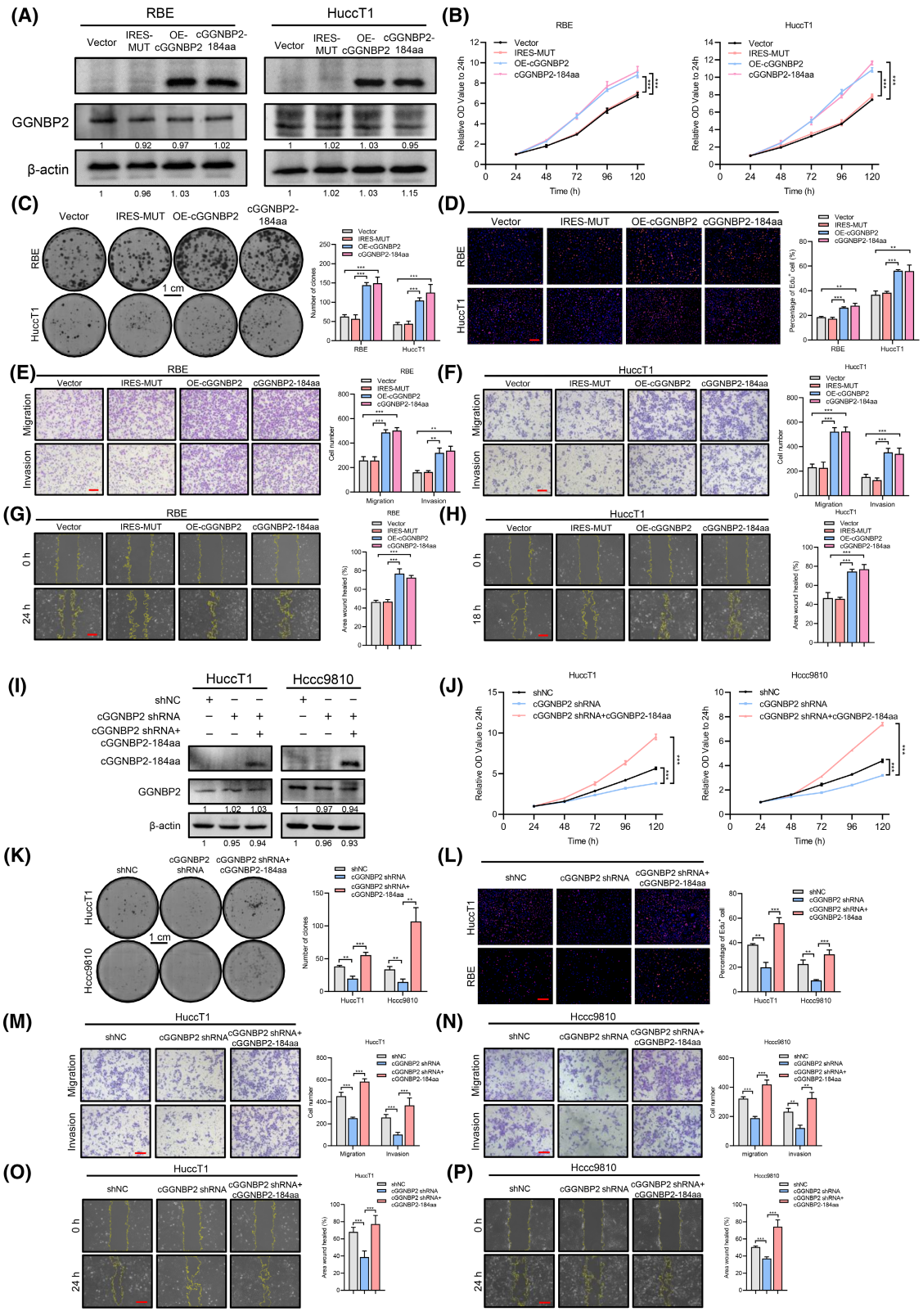

FIGURE 4 cGGNBP2-184aa promotes ICC cell growth and metastasis *in vitro*. (A) Western blotting assays showed the relative cGGNBP2-184aa and GGNBP2 protein expression in indicated cells transfected with four types of vectors. (B-D) cell counting kit-8 (CCK8), colony formation, and 5-ethynyl-2'-deoxyuridine (EDU) assays revealed cell proliferation capacity of indicated ICC cells. Scale bar, 200 μm. (E, F) The migration and invasion capacity were examined in the indicated cells. Scale bar, 200 μm. (G, H) Wound healing assays were performed in the indicated cells. Scale bar, 200 μm. (I) The relative cGGNBP2-184aa and GGNBP2 protein expression in HuccT1 and Hccc9810 cells transfected with negative control shRNA (shNC), cGGNBP2 shRNA, and cGGNBP2-184aa ORF. (J-L) CCK8, colony formation, and EDU assays showed cell proliferation capacity of indicated ICC cells. Scale bar, 200 μm. (M, N) The migration and invasion capacity were examined in the indicated cells. Scale bar, 200 μm. (O, P) Wound healing assays were performed in the indicated cells. Scale bar, 200 μm. $^{**}p < 0.01$; $^{***}p < 0.001$

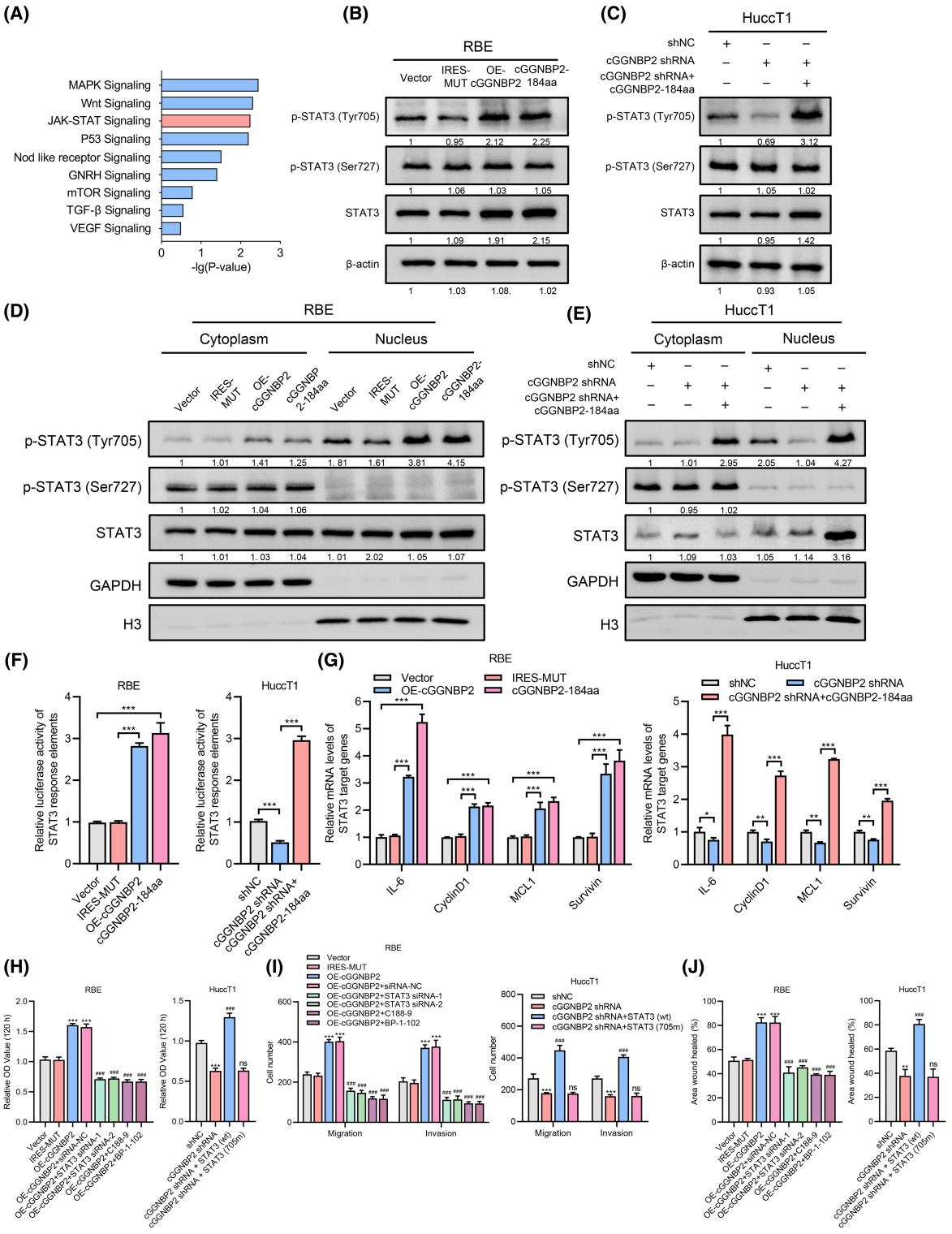

FIGURE 5 cGGNBP2-184aa regulates STAT3 phosphorylation to activate JAK-STAT signaling. (A) Kyoto Encyclopedia of Genes and Genomes pathway analysis showed the significantly affected signaling pathway on cGGNBP2-184aa overexpression in RBE cells. (B, C) Western blotting analysis showed the phosphorylation status of $STAT3^{Tyr705}$ and $STAT3^{Ser727}$ in the indicated cells. (D, E) Subcellular fractionation assays revealed the distribution of phosphorylated $STAT3^{Tyr705}$ and phosphorylated $STAT3^{Ser727}$ in the indicated cells. GAPDH and H3 were used as positive controls in the cytoplasm and nucleus, respectively. (F) Luciferase assays determined the activity of STAT3 response elements in the indicated cells. (G) qRT-PCR analysis for the relative mRNA expression of STAT3 target genes in the indicated cells. (H) Left: cell counting kit-8 (CCK8) assays showed cell proliferation capacity of the indicated cells cotransfected with STAT3 siRNA or treated with C188-9 (20 μM) or BP-1-102 (20 μM). Right: Cell proliferation capacity of the indicated cells cotransfected with wild-type or Tyr705-mutated STAT3 vectors. (I) The migration and invasion capacity were examined in the indicated cells. (J) Wound healing assays were performed in the indicated cells. C188-9 and BP-1-102 were small molecular inhibitor of STAT3. $^{*}p < 0.05$; $^{**}p < 0.01$; $^{***}p < 0.001$; $^{\#\#\#}p < 0.001$ versus OE-cGGNBP2+siRNA-NC or cGGNBP2 shRNA; ns, not significant versus cGGNBP2 shRNA

phosphorylated STAT3^{Tyr705}, whereas nuclear expression of phosphorylated STAT3^{Ser727} and total STAT3 did not (Figure 5D). Consistent with this, overexpression of cGGNBP2-184aa ORF in cGGNBP2 knockdown cells restored nuclear distribution of phosphorylated STAT3^{Tyr705} without changing STAT3^{Ser727}. Interestingly, nuclear expression of total STAT3 was significantly increased after enhancing cGGNBP2-184aa expression in cGGNBP2 silenced HuccT1 cells (Figure 5E). Taken together, our data suggest that cGGNBP2-184aa promotes STAT3^{Tyr705} phosphorylation, nuclear translocation, and activation of the JAK-STAT pathway.

To further confirm the activation of JAK-STAT pathway by cGGNBP2-184aa overexpression, we performed dual-luciferase reporter assays to measure luciferase activity of STAT3 response elements. As expected, increased cGGNBP2-184aa expression significantly enhanced the activity of STAT3 response elements. Restoration of cGGNBP2-184aa level greatly abolished the inhibitory effect of cGGNBP2 silencing on luciferase activity of STAT3 elements in HuccT1 cells (Figure 5F). Furthermore, the mRNA expression levels of STAT3 target genes were also inhibited by cGGNBP2 silencing and restored by overexpression of cGGNBP2-184aa ORF (Figure 5G). Given previous studies have reported that IL-6 treatments could enhance phosphorylation of STAT3 at Tyr705, we examined the STAT3^{Tyr705} phosphorylation in ICC cells treated with IL-6 for various concentrations and time. STAT3^{Tyr705} phosphorylation gradually elevated along with increased IL-6 concentration (Figure S14C). However, cGGNBP2-184aa knockdown abolished the stimulative effect of IL-6 on STAT3^{Tyr705} phosphorylation (Figure S14D). Furthermore, cGGNBP2-184aa knockdown also eliminated the IL-6–induced JAK-STAT signaling activation (Figure S14E,F).

To determine the function of cGGNBP2-184aa–enhanced STAT3^{Tyr705} phosphorylation, we knocked down STAT3 expression with siRNAs and inhibited STAT3^{Tyr705} phosphorylation by chemical inhibitors (C188-8 or BP-1-102) in cGGNBP2-184aa–overexpressed RBE cells (Figure S15A-C). cGGNBP2-184aa–enhanced cell proliferation, migration, and invasion could be abrogated by STAT3 knockdown or inhibition of STAT3^{Tyr705} phosphorylation (Figure 5H-J, left, Figure S16A,B). Moreover, a wild-type or Tyr705-mutated STAT3 plasmid was transfected into cGGNBP2-silenced HuccT1 cells (Figure S15D). The phosphorylation of STAT3^{Tyr705} could be restored by transfecting of wild-type STAT3 and thereafter abolished the inhibitory effect of cGGNBP2 deficiency on cell phenotype. However, cellular growth and metastasis did not show significant alteration after transfection of STAT3 mutant in HuccT1 cells (Figure 5H-J, right, Figure S16C,D). Collectively, our data indicated that IL-6/cGGNBP2-184aa/STAT3 formed a positive feedback loop.

cGGNBP2-184aa interacts with STAT3 to promote its transcriptional activity

To better elucidate the mechanisms that cGGNBP2-184aa up-regulated STAT3^{Tyr705} phosphorylation, we performed immunoprecipitation using an antibody against HA after transfecting HA-labeled cGGNBP2-184aa in RBE cells. After staining with Coomassie blue, the specific proteins pulled down by HA were subjected to mass spectrometry. Apart from bait protein HA-cGGNBP2-184aa, STAT3 was also identified, indicating a potential interaction between cGGNBP2-184aa and STAT3 (Figure 6A). Subsequent co-immunoprecipitations confirmed their mutual interaction (Figure 6B). In addition, immunofluorescence staining validated the colocalization of cGGNBP2-184aa and STAT3 in the cytoplasm of ICC cells (Figure 6C).

To delineate the domains of STAT3 responsible for its interaction with cGGNBP2-184aa, a series of Flag-tagged STAT3 deletion mutants were generated (Figure 6D, left). Following co-immunoprecipitation experiments combined with immunoblotting demonstrated that the DNA binding domain (DBD) of STAT3 was required for the interaction between STAT3 and cGGNBP2-184aa (Figure 6D, right). In the reciprocal analysis, we also determined the regions of cGGNBP2-184aa involved in the STAT3-cGGNBP2-184aa interaction by co-immunoprecipitation with HA-tagged truncation mutants of cGGNBP2-184aa. Only cGGNBP2-184aa$^{[62\text{-}122]}$ could be pulled down by STAT3, indicating that cGGNBP2-184aa interacted with STAT3 through region 62-122 (Figure 6E).

We next tested whether the binding region of cGGNBP2-184aa was responsible for the activation of JAK-STAT signaling. The STAT3^{Tyr705} phosphorylation was remarkably increased by cGGNBP2-184aa expression$^{[62\text{-}122]}$, and total STAT3 expression was slightly enhanced in ICC cells (Figure 6F). The luciferase activity of STAT3 response elements and the mRNA expression of STAT3 downstream genes were enhanced by cGGNBP2-184aa$^{[62\text{-}122]}$ rather than other truncation mutants (Figure 6G,H). Notably, cGGNBP2-184aa–induced cell proliferation and invasion were also attributed to the interaction region of cGGNBP2-184aa (Figure S17A-C). Taken together, cGGNBP2-184aa interacted with the DBD of STAT3 to activate JAK-STAT signaling and promote cellular proliferation and metastasis.

In vivo effects of cGGNBP2-184aa and clinical relevance

Because of cGGNBP2-184aa's crucial role in the activation of JAK-STAT pathway and in vitro promoting cellular phenotypes, we next evaluated whether cGGNBP2-184aa facilitated tumor growth and metastasis in vivo.

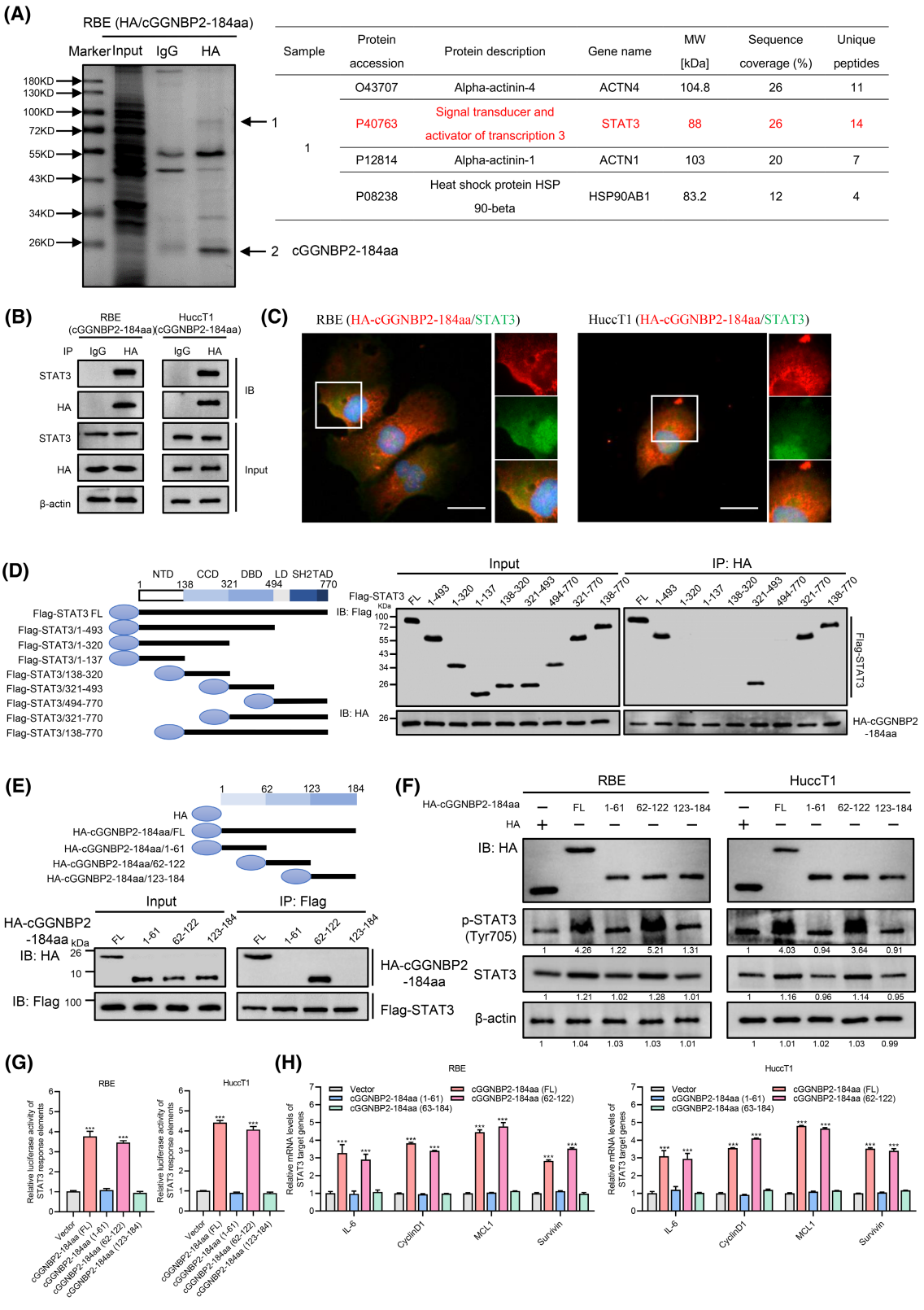

Sample	Protein accession	Protein description	Gene name	MW [kDa]	Sequence coverage (%)	Unique peptides
1	O43707	Alpha-actinin-4	ACTN4	104.8	26	11
	P40763	Signal transducer and activator of transcription 3	STAT3	88	26	14
	P12814	Alpha-actinin-1	ACTN1	103	20	7
	P08238	Heat shock protein HSP 90-beta	HSP90AB1	83.2	12	4

Subcutaneous xenograft models demonstrated that cGGNBP2-184aa overexpression, but not cGGNBP2, accelerated tumor growth (Figure 7A). Overexpression of IRES-MUT cGGNBP2 did not phosphorylate STAT3 in xenografts. In comparison, ectopic cGGNBP2-184aa dramatically promoted the expression of Ki-67 and the phosphorylation level of STAT3 (Figure 7B,D). Furthermore, liver orthotopic-implantation and lung metastasis models were established to test the effect of cGGNBP2-184aa on metastatic capacity. Intrahepatic

FIGURE 6 cGGNBP2-184aa interacts with STAT3 to promote its transcriptional activity. (A) Left: Total proteins were extracted from RBE cells transfected with HA-tagged cGGNBP2-184aa coimmunoprecipitated with antibody against HA and separated through SDS-PAGE, followed by Coomassie brilliant blue staining. The specific bands of interest (shown as arrows) were subjected to mass spectrometric analysis. Right: The table shows mass spectrometric results identifying interaction proteins of cGGNBP2-184aa. (B) Co-immunoprecipitation (co-IP) assays indicate the interaction between cGGNBP2-184aa and STAT3 in RBE and HuccT1 cells transfected with HA-tagged cGGNBP2-184aa. (C) IF assays showed colocation of cGGNBP2-184aa and STAT3 in ICC cells transfected with HA-tagged cGGNBP2-184aa. Scale bar, 10 μm. (D) Left: Schematic of domain structure of STAT3 and Flag-tagged STAT3 mutants. Right: HEK293T cells were transfected with HA-tagged cGGNBP2-184aa and Flag-tagged full-length or STAT3 fragments, followed by immunoprecipitation (IP) using anti-HA antibody. (E) Top: Schematic diagrams showed the wild-type cGGNBP2-184aa and its truncation mutants. Bottom: HEK293T cells were transfected with Flag-tagged STAT3 and HA-tagged cGGNBP2-184aa mutants, followed by IP with anti-Flag antibody. (F) Western blotting assays showed expression levels of phosphorylated $STAT3^{Tyr705}$ and total STAT3 in cells after transfection of wild-type cGGNBP2-184aa ORF or truncation mutants. (G) Luciferase assays showed the activity of STAT3 response elements. (H) qRT-PCR analysis for the relative mRNA expression of STAT3 target genes. CCD, coiled-coil domain; FL, full-length; LD, linker domain; MW, molecular weight; NTD, N-terminal domain; SH2, Src homology 2 protein domain; TAD, transcriptional activation domain. ***$p < 0.001$ versus vector

metastases were remarkably increased by cGGNBP2-184aa overexpression (Figure 7C). In addition, the luciferase activities were much stronger in groups that overexpressed cGGNBP2-184aa than those of negative control or IRES-MUT overexpressed ones (Figure 7E). Lungs were harvested and subjected to H&E staining. Consistently, the numbers of lung metastases were much higher in cGGNBP2-184aa elevated groups (Figure 7F), suggesting that enhanced cGGNBP2-184aa expression promoted lung metastasis of ICC cells. Administration of STAT3 inhibitor could abolish the vast majority of the effect of cGGNBP2-184aa on promoting ICC cell growth and metastasis in vivo (Figure S18).

To further evaluate the clinical utility of cGGNBP2-184aa in ICC progression, we examined the $STAT3^{Tyr705}$ phosphorylation level in 136 patients with ICC and assessed its association with the cGGNBP2 level. A significantly positive correlation was observed between cGGNBP2 and $STAT3^{Tyr705}$ phosphorylation in ICC tissues (Figure 7G,H). Next, we assessed the percentage of tumor-infiltrating lymphocytes (TILs) and found that the proportion of infiltrating inflammatory immune cells was variable in ICC tissues (Figure S19). The correlation was analyzed between TILs and serum IL-6, IL-8, and IL-10 as well as TNF-α levels. The results demonstrated that only serum IL-6 was significantly correlative to TILs in ICC tissues, implying the IL-6 increase was not a mere secondary epiphenomenon of the immune-response associated to ICC. Interestingly, a significant correlation was observed between cGGNBP2 expression levels and intratumoral TILs (Figure 7I).

Finally, we examined the IL-6/cGGNBP2 axis in in vivo assays by administrating recombinant IL-6 and neutralizing IL-6 antibody after being subcutaneously injected with RBE or HuccT1 cells. Tumor growth was accelerated after administration of IL-6, which could be abolished by IL-6 neutralizing antibody (Figure S20A). The xenografts were harvested and measured for the expression of cGGNBP2-184aa, phosphorylated $STAT3^{Tyr705}$, and key genes related to tumor cell growth (Figure S20B). Consistent with in vitro results, IL-6 stimuli increased cGGNBP2-184aa expression and $STAT3^{Tyr705}$ phosphorylation whereas inhibited apoptotic program in vivo. Administration of IL-6 neutralizing antibody could reverse the effect of recombinant IL-6.

DISCUSSION

Accumulating evidence has emphasized the connection between inflammation and cancer progression.[27] IL-6, a multifunctional cytokine, was found overexpressed in various tumors and regulated cancer hallmarks, including proliferation, invasion, and metastasis.[28] Consistent with previous findings, we demonstrated elevated serum IL-6 levels were significantly correlated to more aggressive tumor characteristics and poor prognosis in ICC. We hypothesized that IL-6 could induce the expression of circRNAs to promote ICC progression. To test this hypothesis, high-throughput sequencing was performed. Then, we identified IL-6−induced cGGNBP2, which could encode the protein cGGNBP2-184aa. Ectopic cGGNBP2-184aa expression facilitated ICC cell growth and metastasis in vitro and in vivo. Importantly, cGGNBP2-184aa directly interacted with STAT3 and enhanced its phosphorylation at Tyr705 site, which thereafter translocated into nuclear to activate transcription of target genes.

CircRNAs are a class of covalently closed and endogenous biomolecules whose biogenesis is regulated by trans-acting factors and specific cis-acting elements.[29] Although not fully elucidated, previous studies revealed some RBPs were involved in the biogenesis of circRNAs.[16] In this study, we found that DHX9, a nuclear RNA helicase, showed an inhibitory effect on cGGNBP2 biogenesis by binding to the flanking inverted complementary sequences, which was consistent with previous findings of DHX9's functions.[9] More importantly, we demonstrated that the expression of DHX9 was down-regulated by IL-6 stimuli. However, a previous study has reported that DHX9 expression was enhanced in tumor tissues of hepatocellular carcinoma, suggesting an oncogenic role of DHX9 in hepatocellular carcinoma progression.[11] Therefore, the

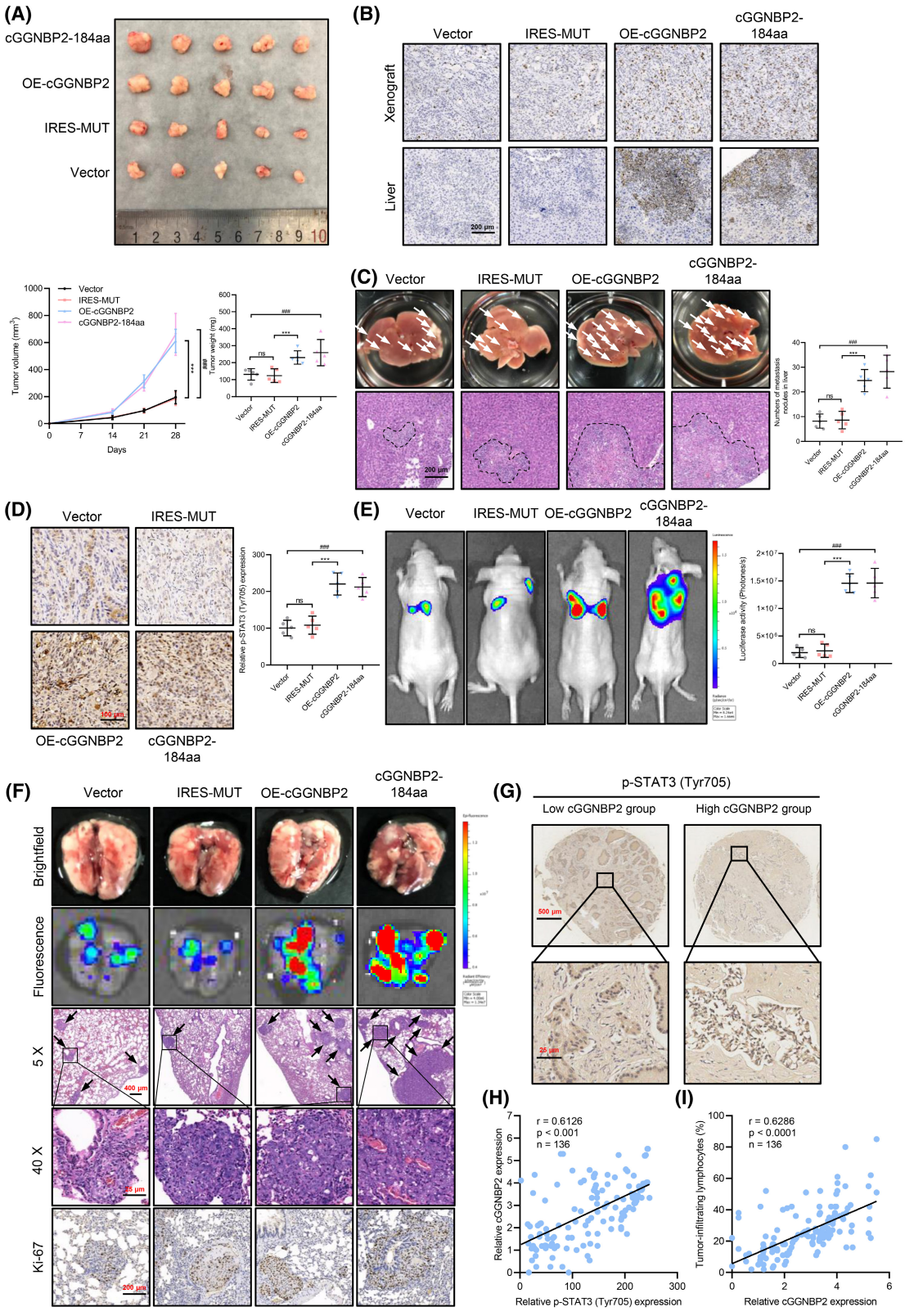

further mechanisms underlying IL-6 down-regulated DHX9 expression, and the role of DHX9 in other cancers requires further investigation.

The biological functions of circRNAs have been intensively described in various cancers. Most circRNAs have been proposed to function as a microRNA sponge or protein scaffold.[30] Recently, increasing evidence has identified a limited number of translatable circRNAs, which could encode regulatory proteins or peptides to modulate cancer progression.[31] Sharing

FIGURE 7 cGGNBP2-184aa promotes tumor growth and metastasis *in vivo*. (A) Tumor volume and weight of subcutaneous xenografts in nude mice injected with indicated RBE cells. (B) Representative images of immunohistochemistry staining of Ki-67 in xenografts and livers. (C) Left, top: Representative images of tumor metastatic foci (white arrows) formed in the livers of nude mice implanted with indicated RBE cells in different groups. Left, bottom: Representative hematoxylin and eosin (HE) staining of metastatic lesions in the livers. Right: Relative statistical analysis of the number of metastatic foci in livers between different groups. (D) Representative images of immunohistochemistry staining of p-STAT3 (Tyr705) in xenografts (left) and relative statistical analysis (right). (E) Left: Representative bioluminescent images of lungs for each experimental group after injection of indicated RBE cells through tail vein. Right: Statistical analysis of bioluminescent tracking plots. (F) Top: Representative lungs and relative fluorescence images. Middle: Representative HE staining of metastatic lesions (black arrows) in the lungs. Bottom: Representative images of immunohistochemistry staining of Ki-67 in lungs. (G) Representative images of immunohistochemistry staining of p-STAT3 (Tyr705) in patients with low or high cGGNBP2 expression. (H) Correlation between the relative cGGNBP2 expression and relative p-STAT3 (Tyr705) expression of tumor tissues from 136 patients with ICC. (I) Correlation between the relative cGGNBP2 expression and TILs in 136 ICC tissues. ***$p < 0.001$ versus IRES-MUT; ###$p < 0.001$ versus Vector; ns, no significance

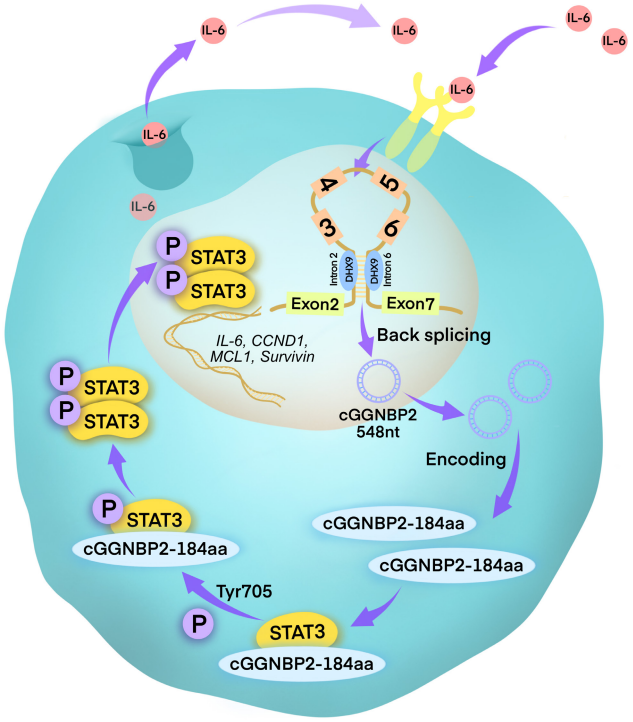

FIGURE 8 Summary figure of the mechanism of cGGNBP2 facilitates tumor progression of ICC. IL-6 stimulation induces the up-regulation of cGGNBP2 (generated from exon 3-6 of *ggnbp2*). The biogenesis of cGGNBP2 is regulated by DHX9 through binding to the flanking inverted complementary sequences. cGGNBP2 encodes a protein cGGNBP2-184aa. cGGNBP2-184aa interacts with the DBD domain of STAT3, phosphorylates its Thy705 site, and initiates the transcription of downstream target genes of STAT3. The IL-6/cGGNBP2-184aa/STAT3 formed a positive feedback loop to sustain ICC growth and metastasis

a majority of amino acid sequences with those of host genes, circRNA-encoded proteins could function as auxiliaries for their linear counterparts. For instance, circSHPRH-146aa shared 131 amino acids with full-length SHPRH and functioned as a protector that prevented degradation of SHPRH protein.[22] In addition, several circRNA-encoded proteins played independent or even opposite roles compared with their linear counterparts.[32] Herein, we demonstrated that cGGNBP2 could encode a functional protein cGGNBP2-184aa. More importantly, cGGNBP2-184aa, rather than cGGNBP2, facilitated cancer hallmarks of ICC. Additionally, we found that the expression of cGGNBP2 was contrary to that of full-length GGNBP2 (data not shown), which implied that cGGNBP2-184aa probably exerted a contrary biological function to GGNBP2. Hence, the mechanisms underlying modulation of back splicing with linear alternative splicing of GGNBP2 and the biological functions of their relative products need further exploration.

Aberrant activations of JAK-STAT signaling has been demonstrated in ICC.[33] IL-6 could be secreted in response to inflammatory stimuli in a paracrine or autocrine manner. In turn, the signal transduction of IL-6 activated JAK-STAT pathway and initiated the transcription of various genes including myeloid cell leukemia 1, cyclin D1, and *IL-6*. The modulation of IL-6/JAK-STAT3 could be mediated by cytokine signaling suppressor of cytokine signaling.[34] Recent studies have showed that long noncoding RNAs and microRNAs could be induced on IL-6 exposure and promoted tumor aggressiveness through epithelial-mesenchymal transition induction.[6,35] However, the potential association between IL-6 and circRNAs remains unclear. Our findings revealed that IL-6–induced cGGNBP2 encoded the protein cGGNBP2-184aa and activated JAK-STAT signaling pathway in ICC cells. Interestingly, silencing STAT3 did not abolish the enhanced effect of IL-6 on cGGNBP2-184aa expression, and cGGNBP2-184aa knockdown could abrogate the effect of IL-6 on JAK-STAT signaling activation, suggesting cGGNBP2-184aa may be upstream of STAT3. Several previous studies have reported long noncoding RNAs could bind to the DBD or C-terminal domain of STAT3 to regulate its phosphorylation status and alter nuclear import-export dynamics.[24,36] Here, we demonstrated that cGGNBP2-184aa directly interacted with the DBD of STAT3 and phosphorylated STAT3 at Tyr705 site. Thereafter, phosphorylated $STAT3^{Tyr705}$ formed homodimerization and translocated into nucleus to initiate transcription of target genes, thereby forming an IL-6–triggered positive feedback loop of IL-6/cGGNBP2-184aa/STAT3 to

promote ICC progression. Currently, therapeutic strategies targeting IL-6/STAT3 pathway in cancers mainly involve directly targeting IL-6 using neutralizing antibodies, such as siltuximab,[37] and directly targeting IL-6R with tocilizumab[38] and inhibitors for STAT3.[39] Although the preclinical use of IL-6/STAT3-targeting agents showed antitumor effects in vitro and in vivo, other predictive biomarkers or specifically functional proteins were still needed in order to rationally incorporate IL-6/STAT3-targeting agents into multimodality therapeutic strategies.[40] Accordingly, given the unusual expression patterns of cGGNBP2, interventions for circRNA cGGNBP2 or cGGNBP2-184aa may provide auxiliary benefits for IL-6/STAT3-targeting agents in ICC.

In summary, our research characterized a IL-6–induced circRNA cGGNBP2. The biogenesis of cGGNBP2 was mediated by RBP DHX9, which was also regulated on IL-6 stimulation. Furthermore, cGGNBP2 encoded the protein cGGNBP2-184aa, which physically interacted with STAT3 and was crucial for $STAT3^{Tyr705}$ phosphorylation. cGGNBP2-184aa facilitated ICC cell growth and metastasis in vitro and in vivo. The IL-6/cGGNBP2-184aa/STAT3 formed a positive feedback loop to sustain the constitutive activation of IL-6/STAT3 signaling in ICC (Figure 7H). Our findings uncovered a mechanism underlying IL-6–induced tumor progression and might suggest an auxiliary target for clinical IL-6/STAT3-targeting treatments in ICC.

ACKNOWLEDGMENTS

We are most grateful for Yan Wang, Jinkui Pi, and Bo Su from Core Facility of West China Hospital and Yang Yang and Xijing Yang from the Animal Experimental Center of West China Hospital for their technique support. Shiyang Zheng from the Third Affiliated Hospital of Guangzhou Medical University, Haizhou Qiu from West China Hospital, and Xin Huang from University of Pittsburgh School of Medicine for their support in revising the paper. We also thank West China Biobanks at Department of Clinical Research Management in West China Hospital for the continuous support.

AUTHOR CONTRIBUTIONS

Conceptualization: Hong Wu and Yong Zeng; data curation: Hui Li, Tian Lan, Hailing Liu, Chang Liu, Junlong Dai, and Lin Xu; formal analysis: Hui Li, Tian Lan, Hailing Liu, Lin Xu, and Kefei Yuan; methodology: Hui Li, Yunshi Cai, Guimin Hou, Kunlin Xie, Mingheng Liao, Jiaxin Li, and Jiwei Huang; critical revision of the manuscript: Hong Wu, Genshu Wang, and Kefei Yuan; funding acquisition: Hong Wu, Yong Zeng and Kefei Yuan; supervision: Hong Wu, Yong Zeng, Genshu Wang, and Kefei Yuan; writing – original draft: all authors; revised paper: all authors.

REFERENCES

1. Sung H, Ferlay J, Siegel RL, Laversanne M, Soerjomataram I, Jemal A, et al. Global cancer statistics 2020: GLOBOCAN estimates of incidence and mortality worldwide for 36 cancers in 185 countries. CA Cancer J Clin. 2021;71(3):209–49.
2. Valle JW, Kelley RK, Nervi B, Oh DY, Zhu AX. Biliary tract cancer. Lancet. 2021;397(10272):428–44.
3. Blechacz B, Komuta M, Roskams T, Gores GJ. Clinical diagnosis and staging of cholangiocarcinoma. Nat Rev Gastroenterol Hepatol. 2011;8(9):512–22.
4. Fidler IJ. The pathogenesis of cancer metastasis: the 'seed and soil' hypothesis revisited. Nat Rev Cancer. 2003;3(6):453–8.
5. Balkwill F, Mantovani A. Inflammation and cancer: Back to Virchow? Lancet. 2001;357(9255):539–45.
6. Wu J, Zhang J, Shen B, Yin K, Xu J, Gao W, et al. Long noncoding RNA lncTCF7, induced by IL-6/STAT3 transactivation, promotes hepatocellular carcinoma aggressiveness through epithelial-mesenchymal transition. J Exp Clin Cancer Res. 2015;34(1):116.
7. Memczak S, Jens M, Elefsinioti A, Torti F, Krueger J, Rybak A, et al. Circular RNAs are a large class of animal RNAs with regulatory potency. Nature. 2013;495(7441):333–8.
8. Kristensen LS, Andersen MS, Stagsted LVW, Ebbesen KK, Hansen TB, Kjems J. The biogenesis, biology and characterization of circular RNAs. Nat Rev Genet. 2019;20(11):675–91.
9. Liu H, Lan T, Li H, Xu L, Chen X, Liao H, et al. Circular RNA circDLC1 inhibits MMP1-mediated liver cancer progression via interaction with HuR. Theranostics. 2021;11(3):1396–411.
10. Yu J, Xu QG, Wang ZG, Yang Y, Zhang L, Ma JZ, et al. Circular RNA cSMARCA5 inhibits growth and metastasis in hepatocellular carcinoma. J Hepatol. 2018;68(6):1214–27.
11. Lei M, Zheng G, Ning Q, Zheng J, Dong D. Translation and functional roles of circular RNAs in human cancer. Mol Cancer. 2020;19(1):30.
12. Yang Y, Wang Z. IRES-mediated cap-independent translation, a path leading to hidden proteome. J Mol Cell Biol. 2019;11(10):911–9.
13. Wu X, Xiao S, Zhang M, Yang L, Zhong J, Li BO, et al. A novel protein encoded by circular SMO RNA is essential for Hedgehog signaling activation and glioblastoma tumorigenicity. Genome Biol. 2021;22(1):33.
14. Gosain R, Anwar S, Miller A, Iyer R, Mukherjee S. Interleukin-6 as a biomarker in patients with hepatobiliary cancers. J Gastrointest Oncol. 2019;10(3):537–45.
15. Høgdall D, O'Rourke CJ, Dehlendorff C, Larsen OF, Jensen LH, Johansen AZ, et al. Serum IL6 as a prognostic biomarker and IL6R as a therapeutic target in biliary tract cancers. Clin Cancer Res. 2020;26(21):5655–67.
16. Okholm TLH, Sathe S, Park SS, Kamstrup AB, Rasmussen AM, Shankar A, et al. Transcriptome-wide profiles of circular RNA and RNA-binding protein interactions reveal effects on circular RNA biogenesis and cancer pathway expression. Genome Med. 2020;12(1):112.
17. Ashwal-Fluss R, Meyer M, Pamudurti N, Ivanov A, Bartok O, Hanan M, et al. circRNA biogenesis competes with pre-mRNA splicing. Mol Cell. 2014;56(1):55–66.
18. Aktaş T, Avşar Ilık İ, Maticzka D, Bhardwaj V, Pessoa Rodrigues C, Mittler G, et al. DHX9 suppresses RNA processing defects originating from the Alu invasion of the human genome. Nature. 2017;544(7648):115–9.
19. Jeck WR, Sorrentino JA, Wang K, Slevin MK, Burd CE, Liu J, et al. Circular RNAs are abundant, conserved, and associated with ALU repeats. RNA. 2013;19(2):141–57.
20. Zhang XO, Wang HB, Zhang Y, Lu X, Chen LL, Yang L. Complementary sequence-mediated exon circularization. Cell. 2014;159(1):134–47.

21. Yang Y, Gao X, Zhang M, Yan S, Sun C, Xiao F, et al. Novel role of FBXW7 circular RNA in repressing glioma tumorigenesis. J Natl Cancer Inst. 2018;110(3):304–15.
22. Zhang M, Huang N, Yang X, Luo J, Yan S, Xiao F, et al. A novel protein encoded by the circular form of the SHPRH gene suppresses glioma tumorigenesis. Oncogene. 2018;37(13):1805–14.
23. Chen X, Han P, Zhou T, Guo X, Song X, Li Y. circRNADb: A comprehensive database for human circular RNAs with protein-coding annotations. Sci Rep. 2016;6(1):34985.
24. Zhang J, Li Z, Liu L, Wang Q, Li S, Chen DI, et al. Long noncoding RNA TSLNC8 is a tumor suppressor that inactivates the interleukin-6/STAT3 signaling pathway. Hepatology. 2018;67(1):171–87.
25. Zhang C, Yue C, Herrmann A, Song J, Egelston C, Wang T, et al. STAT3 activation-induced fatty acid oxidation in CD8(+) T effector cells is critical for obesity-promoted breast tumor growth. Cell Metab. 2020;31(1):148–61.e5.
26. Darnell JE Jr, Kerr IM, Stark GR. Jak-STAT pathways and transcriptional activation in response to IFNs and other extracellular signaling proteins. Science. 1994;264(5164):1415–21.
27. Coussens LM, Werb Z. Inflammation and cancer. Nature. 2002;420(6917):860–7.
28. Ikeguchi M, Hatada T, Yamamoto M, Miyake T, Matsunaga T, Fukumoto Y, et al. Serum interleukin-6 and -10 levels in patients with gastric cancer. Gastric Cancer. 2009;12(2):95–100.
29. Kramer MC, Liang D, Tatomer DC, Gold B, March ZM, Cherry S, et al. Combinatorial control of Drosophila circular RNA expression by intronic repeats, hnRNPs, and SR proteins. Genes Dev. 2015;29:2168–82.
30. Cen J, Liang Y, Huang Y, Pan Y, Shu G, Zheng Z, et al. Circular RNA circSDHC serves as a sponge for miR-127-3p to promote the proliferation and metastasis of renal cell carcinoma via the CDKN3/E2F1 axis. Mol Cancer. 2021;20(1):19.
31. Wu P, Mo Y, Peng M, Tang T, Zhong YU, Deng X, et al. Emerging role of tumor-related functional peptides encoded by lncRNA and circRNA. Mol Cancer. 2020;19(1):22.
32. Liang WC, Wong CW, Liang PP, Shi M, Cao YE, Rao ST, et al. Translation of the circular RNA circβ-catenin promotes liver cancer cell growth through activation of the Wnt pathway. Genome Biol. 2019;20(1):84.
33. Sia D, Tovar V, Moeini A, Llovet JM. Intrahepatic cholangiocarcinoma: Pathogenesis and rationale for molecular therapies. Oncogene. 2013;32(41):4861–70.
34. Isomoto H, Mott JL, Kobayashi S, Werneburg NW, Bronk SF, Haan S, et al. Sustained IL-6/STAT-3 signaling in cholangiocarcinoma cells due to SOCS-3 epigenetic silencing. Gastroenterology. 2007;132(1):384–96.
35. Rokavec M, Öner MG, Li H, Jackstadt R, Jiang L, Lodygin D, et al. IL-6R/STAT3/miR-34a feedback loop promotes EMT-mediated colorectal cancer invasion and metastasis. J Clin Invest. 2014;124(4):1853–67.
36. Wang P, Xue Y, Han Y, Lin LI, Wu C, Xu S, et al. The STAT3-binding long noncoding RNA lnc-DC controls human dendritic cell differentiation. Science. 2014;344(6181):310–3.
37. Coward J, Kulbe H, Chakravarty P, Leader D, Vassileva V, Leinster DA, et al. Interleukin-6 as a therapeutic target in human ovarian cancer. Clin Cancer Res. 2011;17(18):6083–96.
38. Goumas FA, Holmer R, Egberts JH, Gontarewicz A, Heneweer C, Geisen U, et al. Inhibition of IL-6 signaling significantly reduces primary tumor growth and recurrencies in orthotopic xenograft models of pancreatic cancer. Int J Cancer. 2015;137(5):1035–46.
39. Turkson J, Ryan D, Kim JS, Zhang YI, Chen Z, Haura E, et al. Phosphotyrosyl peptides block Stat3-mediated DNA binding activity, gene regulation, and cell transformation. J Biol Chem. 2001;276(48):45443–55.
40. Johnson DE, O'Keefe RA, Grandis JR. Targeting the IL-6/JAK/STAT3 signalling axis in cancer. Nat Rev Clin Oncol. 2018;15(4):234–48.

SUPPORTING INFORMATION

Additional supporting information may be found in the online version of the article at the publisher's website.

How to cite this article: Li H, Lan T, Liu H, Liu C, Dai J, Xu L, et al. IL-6–induced cGGNBP2 encodes a protein to promote cell growth and metastasis in intrahepatic cholangiocarcinoma. Hepatology. 2022;75:1402–1419. https://doi.org/10.1002/hep.32232